

IN SITU SYNTHESIS OF STYRENE-ACRYLIC EMULSION IN THE PRESENCE OF CaCO₃ NANOPARTICLES

X. L. HU^a, Y. J. TANG^{ab*}, Z. Y. YANG^c, Q. Q. PEI^a, Z. J. HU^d, J. H. ZHANG^a,
D. L. GUO^a, N. ZHANG^e

^aNational Engineering Laboratory of Textile Fiber Materials and Processing Technology, Zhejiang Sci-Tech University, Hangzhou 310018, China

^bKey Lab of Pulp and Paper Science & Technology of Ministry of Education, Qilu University of Technology, Jinan 250353, China

^cEngineering Research Center for Eco-Dyeing & Finishing of Textiles, Ministry of Education, Zhejiang Sci-Tech University, Hangzhou 310018, China

^dSchool of Biological and Chemical Engineering, Zhejiang University of Science and Technology, Hangzhou 310023, China

^eShanghai Tonnor Material Science Co., Ltd., Shanghai 200092, China

Organic-inorganic nanocomposites, embodying enhanced properties, e.g., mechanical and thermal properties by combining the advantage of both organic and inorganic moieties, showed great promise in various application areas, such as coatings, cosmetics, catalysis, solar cell, and biology. In the present work, styrene-acrylic emulsion was successfully prepared by in-situ polymerization in the presence of CaCO₃ nanoparticles. The obtained styrene-acrylic/CaCO₃ nanoparticle composite emulsion was structurally characterized by TEM, FT-IR and TGA. Results showed that the styrene-acrylic/CaCO₃ nanoparticle composite emulsion was composed by large amounts of core-shell latex particles, in which CaCO₃ nanoparticles and polymer were employed as core and shell structure, respectively. Moreover, the thermal stability of styrene-acrylic emulsion was greatly improved as a function of the incorporated CaCO₃ nanoparticles. Additionally, related properties, i.e., membrane forming ability, water resistance, ion stability, mechanical stability and storage ability of nanocomposite emulsion in the presence/absence of CaCO₃ nanoparticles were also evaluated.

(Received July 10, 2015; Accepted September 5, 2015)

Keywords: Styrene-acrylic emulsion; In-situ polymerization; CaCO₃ nanoparticles; Core-shell structure; Thermal stability

1. Introduction

In general, organic-inorganic nanomaterials may embody enhanced properties such as mechanical and thermal properties by combining the advantage of both organic and inorganic moieties [1]. These materials may find wide applications in the fields of coatings, cosmetics, catalysis, solar cell, and biology [2, 3]. Styrene-acrylic emulsion, a well-known non-cross-linked emulsion, has shown great potential in various application fields. However, there is still some resistance to wider application of these products, involving low water resistance, poor thermal stability and limited membrane-forming ability. In this sense, the presence of inorganic nanoparticles in the polymerization of styrene-acrylic emulsion might provide an effective approach for imparting improved properties to the resulting products.

*Corresponding author: tangyj@zstu.edu.cn

Inorganic nanoparticles can compound with organic monomer in the polymerization process, which has been an important method of modified polymerization at present due to its simplified operation and almost no effect on original polymerization process. Luo et al. [1] achieved SiO₂/polyacrylate composite films using sol-gel method. It was found that SiO₂/polyacrylate composite films exhibited desirable thermal stability at a dosage of 10 wt% for isopropanol to silica sol. Etmimi et al. [4] obtained exfoliated poly(styrene-butyl acrylate)/GO nanocomposite latex by intercalation polymerization. Graphene oxide nanosheets were exfoliated into about 2~5 layers in the obtained emulsion system. Nanocomposite latex exhibited higher decomposition temperature and thermal stability as compared to the pure poly(styrene-butyl acrylate) latex. In-situ dispersion polymerization is also a common method for preparing the emulsion reinforced by inorganic nanoparticles. The specified nanoparticles were firstly dispersed in monomers prior to the tailored polymerization. Tong et al. [5] synthesized SiO₂/ACR composite emulsion by in-situ emulsion polymerization using nano-SiO₂ particles as core and acrylic resin as shell. It was indicated that the more amount of SiO₂, the less rate of monomer conversion. The composite material, blended with 10% SiO₂ encapsulated ACR and PVC resin, had excellent tensile strength and impact strength in comparison to the pure ACR and PVC resin. Qi et al. [6] investigated the mini-emulsification and mini-emulsion polymerization of methyl methacrylate (MMA) dispersed solution containing nano-SiO₂. It was considered that the modification of nano-SiO₂ could inhibit the escape of nanoparticles from submicron MMA droplets to water phase, thus achieving the combination of inorganic nanoparticles and organic polymers. Overall, variable monomers, e.g., styrene [7, 8], methyl methacrylate [9], acrylonitrile [10], butyl acrylate [11] and vinyl acetate [12], could be used in the process of in-situ emulsion polymerization. Meanwhile, inorganic nanoparticles, e.g., magnetic nano-Fe₃O₄ [13] and nano-SiO₂ [14] may be used in the targeted products.

In the present work, styrene-acrylic emulsion was successfully prepared via in-situ emulsion polymerization process in the presence of CaCO₃ nanoparticles. Moreover, the obtained styrene-acrylic/CaCO₃ nanoparticle composite emulsion was characterized by using various kinds of methods. It was demonstrated that the presence of CaCO₃ nanoparticles could facilitate the production of styrene-acrylic emulsion and reinforce the resulting products. The related properties of the as-prepared products could be improved as a function of the applied CaCO₃ nanoparticles. This work might provide an effective approach for the production of styrene-acrylic emulsion with desired properties.

2. Experimental

2.1 Materials

KH570 modified CaCO₃ nanoparticles were prepared by following the procedure as described in our previous work [15]. Sodium bicarbonate (NaHCO₃), sodium lauryl sulfate (SDS) and anhydrous calcium chloride (CaCl₂) were supplied by Hangzhou Gao Jing fine Chemical Co., Ltd., China. Styrene (St) and methyl methacrylate (MMA) were purchased from Tianjin Municipality Kemi'ou Chemical Reagent Co., Ltd. Butyl acrylate (BA) and alkylphenol polyoxyethylene were purchased from Tianjin Yongda Chemical Reagent Co., Ltd. N-hexadecane and hydroquinone were obtained from Aladdin Reagent Co., Ltd. Ammonium persulfate (APS) was purchased from Hangzhou Mick Chemical Co., Ltd. Distilled water was used for all experiments.

2.2 Preparation of styrene-acrylic/CaCO₃ nanoparticle nanocomposite emulsion

Initially, 0.5 g modified CaCO₃ nanoparticles, 24 g St, 24 g BA and 4.8 g MMA were successively added into a three-neck round-bottomed flask to form a mixture in the presence of

sonication for 5 min. Subsequently, 0.48 g SDS and 0.96 g OP-10 were dispersed into 112 g distilled water, and then was added into the above flask and stirred for pre-emulsion. Afterwards, 0.29 g n-hexadecane was also added to the emulsion. After increasing the temperature to 70 °C, 0.6 g APS and 0.5 g NaHCO₃ were added as initiator and pH regulator, respectively. Subjected to mechanical stirring for 5 h, the desired styrene-acrylic/CaCO₃ nanoparticle nanocomposite emulsion was obtained.

2.3 Calculation of monomer conversion rate

Adequate emulsion was added into a weighing bottle, weighed immediately, then 1~2 drops of hydroquinone was added to the emulsion as flame retardant. The above mixture was oven-dried at 105 °C up to a constant weight. As a result, monomer conversion rate was calculated by using the following Eqs.:

$$\omega_s = \frac{M_f - M_0}{M_s - M_0} \times 100\% \quad (1)$$

$$\omega_c = \frac{M_t \times \omega_s - M_n}{M_M} \quad (2)$$

In Eq. (1), ω_s represents solid content, M_0 is the mass of weighing bottle, M_s denotes the total mass of styrene-acrylic/CaCO₃ nanoparticle nanocomposite emulsion for oven-drying and weighing bottle, and M_f denotes the total mass of oven-dried styrene-acrylic/CaCO₃ nanoparticle nanocomposite emulsion and weighing bottle.

In Eq.(2), ω_c represents monomer conversion rate, M_t is total mass of styrene-acrylic/CaCO₃ nanoparticle nanocomposite emulsion; M_n is total mass of non-volatile materials; M_M is total mass of polymeric monomer.

2.4. Stability evaluation of styrene-acrylic/CaCO₃ nanoparticle nanocomposite emulsion

2.4.1 Calcium ion stability

The ability of polymerization emulsion bearing electrolytes was termed as ion stability, called chemical stability as well. It is usually measured with calcium ion. Specifically, 16 mL styrene-acrylic/CaCO₃ nanoparticle nanocomposite emulsion and 4 mL 0.5% CaCO₃ suspension were added into a 20 mL calibration test-tube and underwent shaking prior to rest for 48 h. Ion stability is identified by means of gel and stratification. Calcium stability is available if there are no gel and stratification phenomenon. If stratification appears, it is necessary to measure the height of clear liquid. The higher height of clear liquid means the poorer calcium ion stability of styrene-acrylic/CaCO₃ nanoparticle nanocomposite emulsion.

2.4.2 Mechanical stability

10 mL styrene-acrylic/CaCO₃ nanoparticle nanocomposite emulsion was added into a centrifuge tube and stirred for 0.5 h at a stirring rate of 4000 rpm.

2.4.3 Storage stability

Visual form of styrene-acrylic/CaCO₃ nanoparticle nanocomposite emulsion was observed after rest for three months.

2.5. Water resistance of emulsion membrane

Styrene-acrylic/CaCO₃ nanoparticle nanocomposite emulsion was coated on the surface of a glass plate, air-dried, and then put into water slowly. Foaming time was observed and recorded. It is well known that the longer time, the better water resistance.

2.6. Analysis and characterization

Thermo gravimetric analysis (TGA) of nanoparticle nanocomposite styrene-acrylic emulsion thin film was carried out under nitrogen atmosphere using PYRIS 1 type thermo gravimetric analyzer (USA). The temperature was increased from 25 °C to 750 °C at a heating rate of 10 °C/min. Fourier-transformed infrared (FT-IR) spectra of styrene-acrylic/CaCO₃ nanoparticle nanocomposite emulsion was collected using a Nicolet 5700 FT-IR spectrometer. Particle size distribution of the conventional styrene-acrylic emulsion and styrene-acrylic/CaCO₃ nanoparticle nanocomposite emulsion were determined by using LB-550 type particle size analyzer (Horiba, Japan). The microstructure was observed based on JEM-2100 type transmission electron microscopy (TEM) (JEOL, Japan).

3. Results and discussion

3.1. Effect of emulsifier amount on monomer conversion rate

Emulsifier is dispersed into distilled water in the form of special “micellar”. It mainly plays a role of dispersion, stability and solubilization in the process of polymerization [16]. Among them, nonionic emulsifier could enhance emulsion stability for resisting pH value, inorganic salt and freeze-thaw due to steric effect and shielding effect. Anionic emulsifier, which could disperse and stabilize emulsion with the double electronic shell, has strong emulsifying capacity. As a consequence, they are usually used together, which could exert synergetic effect and efficiently enhance comprehensive properties of resulting emulsion [17].

In the present work, at SDS: OP-10=1: 2, effect of emulsifier amount on the monomer conversion was studied, and the results are shown in Fig. 1. As can be seen, monomer conversion rate increased with the increased emulsifier amount. It can be noted that the maximum conversion rate (98%) was reached when emulsifier amount was located at 3%. Monomer conversion rate remained constant with a further increase in emulsifier amount. In this regard, optimum amount of emulsifier was controlled at 3%.

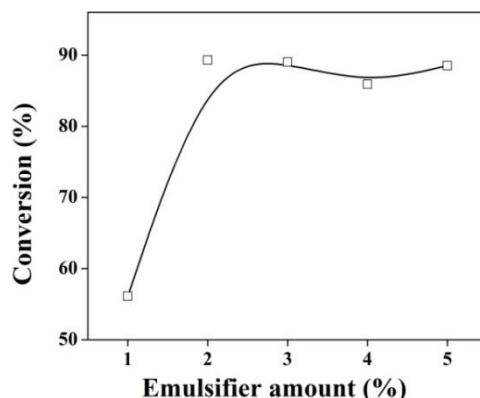


Fig. 1. Monomer conversion rate as a function of emulsifier amount
(The ratio of SDS to OP-10 was 1:2)

3.2. Effect of CaCO₃ nanoparticle amount on monomer conversion rate

Fig. 2 demonstrates the effect of CaCO₃ nanoparticle amount on monomer conversion rate. It can be seen that there was no significant effect on overall trend of emulsion polymerization in the presence of CaCO₃ nanoparticles. The monomer conversion rate increased gradually with the prolonged time, and then trended toward a constant value of about 90%. However, monomer conversion rate was decreased with increased CaCO₃ nanoparticle amount, especially in the initial stage. It may be largely related to the inhibition of CaCO₃ nanoparticle. Polymerization reaction was free radical reaction, and a few electric charges of surface of CaCO₃ nanoparticles can react with free radicals, which reduced efficiency of initiators, thus resulting in a slow increase of polymer chain. By comprehensive consideration, optimum amount of CaCO₃ nanoparticle was set at 1%.

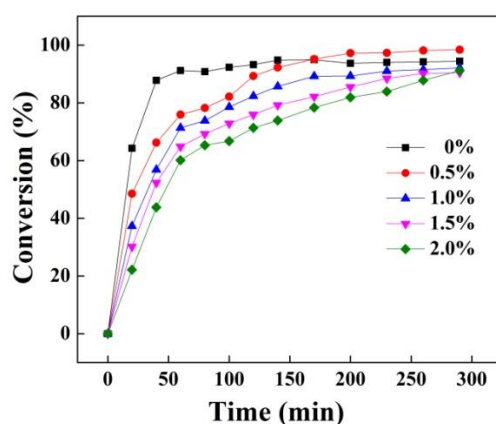


Fig. 2. Monomer conversion rate as a function of CaCO₃ nanoparticle amount
(The emulsifier amount was 3%)

3.3. TEM observations

TEM was used to confirm that the CaCO₃ nanoparticles were encapsulated in emulsion particles, and the typical TEM images of conventional styrene-acrylic emulsion and styrene-acrylic/CaCO₃ nanoparticle nanocomposite emulsion are compared in Fig. 3. It can be seen in Fig. 3(a) that the conventional emulsion particles exhibited a sphere structure with diameter of about 70 nm. However, Fig. 3(b) indicates that styrene-acrylic/CaCO₃ nanoparticle nanocomposite emulsion exhibited sphere or deformed structure, and the whole particle size was increased to about 120 nm. It can be observed that there was a black point in the emulsion particles, providing direct evidence that styrene-acrylic/CaCO₃ nanoparticle nanocomposite emulsion appeared as a composite core-shell latex particles, in which CaCO₃ nanoparticle and the polymer were employed as core and shell structure, respectively, thereby resulting in the increased particle size.

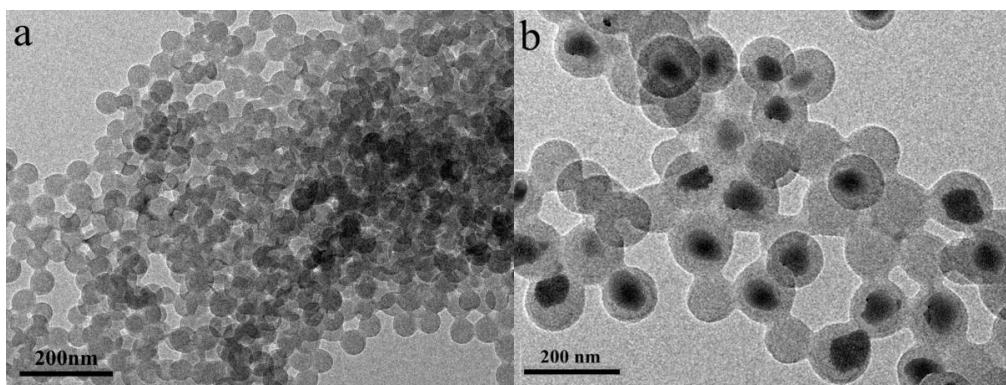


Fig. 3. TEM images of (a) styrene-acrylic emulsion and (b) styrene-acrylic/ CaCO_3 nanoparticle nanocomposite emulsion

3.4. Particle size distribution

The particle size distribution of the conventional styrene-acrylic emulsion and styrene-acrylic/ CaCO_3 nanoparticle nanocomposite emulsion are shown in Fig. 4.

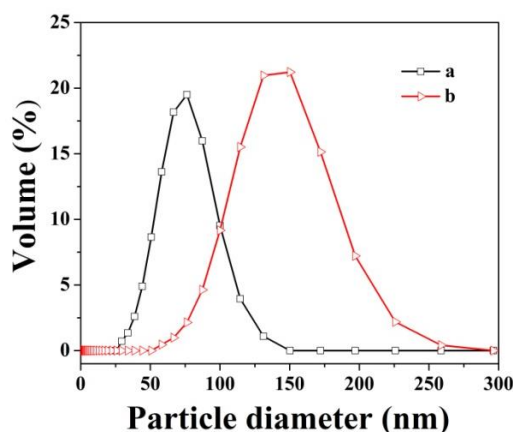


Fig. 4. Particle size distribution of (a) styrene-acrylic emulsion and (b) styrene-acrylic/ CaCO_3 nanoparticle nanocomposite emulsion

It was evident that both samples exhibited a similar particle size distribution. In contrast, the particle size distribution area of styrene-acrylic/ CaCO_3 nanoparticle nanocomposite emulsion seemed to be slightly wider. Specifically, the average particle size of both samples was also obtained. Conventional styrene-acrylic emulsion has an average particle size of 68 nm. In contrast, styrene-acrylic/ CaCO_3 nanoparticle nanocomposite emulsion possessed an average particle size of 130 nm. This result provides further evidence that CaCO_3 nanoparticles were indeed encapsulated in emulsion particles, contributing to form composite latex particles, in which CaCO_3 nanoparticles and the polymer acted as core and shell structure, respectively, thus leading to the increase of the particle size, in good agreement with the observation from TEM images.

3.5. FT-IR spectra

FT-IR spectra of styrene-acrylic/ CaCO_3 nanoparticle nanocomposite emulsion are shown

in Fig. 5. Specifically, the characteristic peaks at 2956cm^{-1} , 2933cm^{-1} and 2874cm^{-1} were due to the stretching vibrations of C-H bands in methyl or methylene groups. The absorption peaks at 3026cm^{-1} and 699cm^{-1} were attributed to benzene ring C-H stretching vibrations and out of plane bending vibrations. The absorption peaks at 1452cm^{-1} , 1494cm^{-1} , 1583cm^{-1} and 1602cm^{-1} were the typical characteristic peaks of benzene ring, which indicated that styrene was successfully participated in the polymerization reaction. In addition, the strong adsorption peak at 1164cm^{-1} belonged to the absorption band of saturated $-\text{C}-\text{C}(=\text{O})-\text{O}-$, and the absorption peak at 1728cm^{-1} was assigned to the carbonyl stretching vibrations, which showed existence of the ester group [15] and further confirmed that styrene-acrylic emulsion has been successfully polymerized.

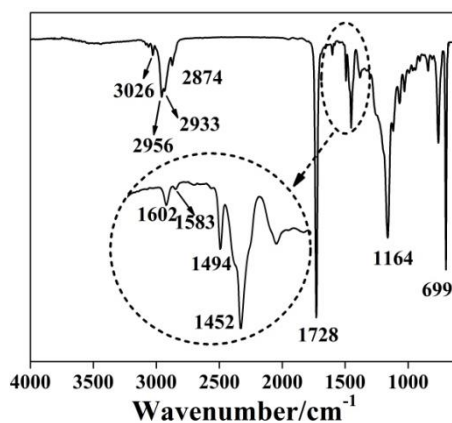


Fig. 5. FTIR spectra of styrene-acrylic/ CaCO_3 nanoparticle nanocomposite emulsion

Based on the proposal of recent literature [18], the possible reaction mechanism of styrene-acrylic/ CaCO_3 nanoparticle nanocomposite emulsion was deduced and demonstrated in Fig. 6. First, KH570 was grafted on the surface of CaCO_3 nanoparticles, which could lead to the enhanced reaction activity of nanoparticles. Afterwards, the targeted composite may be easily obtained by the combination of modified CaCO_3 nanoparticles and styrene-acrylic emulsion via in-situ polymerization.

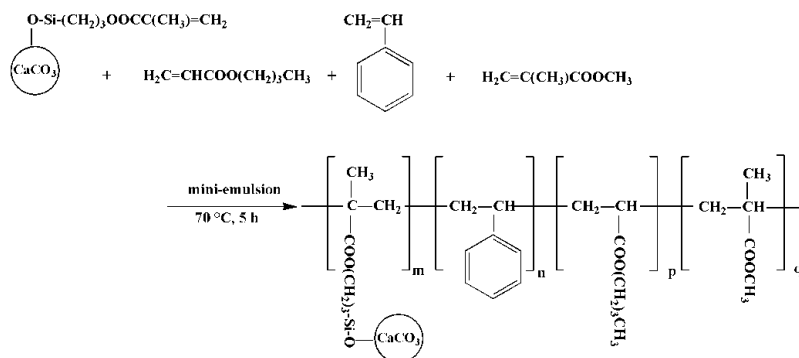


Fig. 6. Molecular design of styrene-acrylic/ CaCO_3 nanoparticle nanocomposite emulsion

3.6. Thermo decomposition behavior

TG curves of the conventional styrene-acrylic emulsion film and styrene-acrylic/ CaCO_3 nanoparticle nanocomposite emulsion film are compared in Fig. 7. It can be seen from Area A, decomposition onset of the conventional emulsion film was at 355 °C, and which value was increased by 8 °C in the presence of CaCO_3 nanoparticles. It can be noted that the temperature range of decomposition of styrene-acrylic/ CaCO_3 nanoparticle nanocomposite emulsion was increased to 87 °C from 82 °C as compared to the conventional emulsion, which indicated the thermal stability of styrene-acrylic/ CaCO_3 nanoparticle nanocomposite emulsion was greatly improved. Area B is the stability area where decomposition of both samples was complete. It can be observed that final residue of styrene-acrylic/ CaCO_3 nanoparticle nanocomposite emulsion was higher (1%) than that of the conventional emulsion, corresponding to the dosage of CaCO_3 nanoparticles.

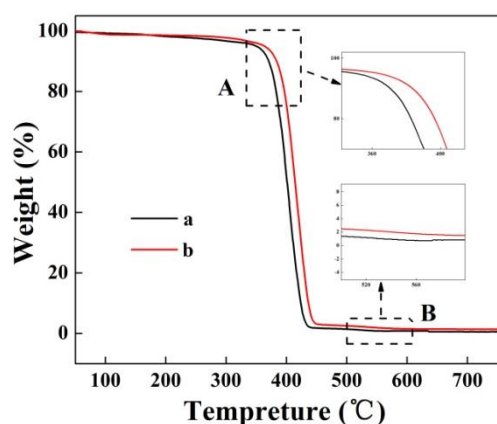


Fig. 7. TG curves of emulsion (a) styrene-acrylic emulsion and (b) styrene-acrylic/ CaCO_3 nanoparticle nanocomposite emulsion

3.7 Other properties evaluation

For overall evaluation of obtained styrene-acrylic/ CaCO_3 nanoparticle nanocomposite emulsion, other related properties, e.g., membrane forming ability, ion stability, water resistance, mechanical stability and storage stability were also considered, and the result are given in Table 1. In general, in comparison to conventional styrene-acrylic emulsions, the water resistance of styrene-acrylic/ CaCO_3 nanoparticle nanocomposite film was pronouncedly improved as a function of the integration of CaCO_3 nanoparticles.

Table 1 Comparative properties between styrene-acrylic/ CaCO_3 nanoparticle nanocomposite emulsion and styrene-acrylic emulsion

Emulsion type	membrane forming ability	water resistance	ion stability	mechanical stability	Storage stability
styrene-acrylic emulsion	good	56 h	available	good	>3 months
styrene-acrylic/ CaCO_3 nanoparticle nanocomposite emulsion	good	83 h	available	good	>3 months

4. Conclusions

In the present work, the synthesis of styrene-acrylic emulsions was performed in the presence of CaCO₃ nanoparticles. Effects of emulsifier and CaCO₃ nanoparticle amount on the monomer conversion rate were highlighted. It was shown that optimum amount of emulsifier and CaCO₃ nanoparticle were 3% and 1%, respectively. The styrene-acrylic/CaCO₃ nanoparticle nanocomposite emulsion was characterized by TEM, particle size distribution, FT-IR and TGA. The results showed that styrene-acrylic/CaCO₃ nanoparticle nanocomposite emulsion exhibited a core-shell structure with an average particle size of 130 nm. It was apparent that CaCO₃ nanoparticle acted as the core and the organic polymer served as the shell, indicating the successful combination between CaCO₃ nanoparticles and styrene-acrylic emulsion. Besides, in comparison to the conventional styrene-acrylic emulsion, the thermal stability and water resistance of styrene-acrylic/CaCO₃ nanoparticle nanocomposite emulsion was greatly improved while other conventional properties were also ensured.

Acknowledgements

This work was financially supported by the National Natural Science Foundation of China (Grant No. 31100442), Zhejiang Provincial Natural Science Foundation of China (Grant No. LY14C160003, LY13C160006), Zhejiang Provincial Top Key Academic Discipline of Chemical Engineering, Technology, Zhejiang Open Foundation of the Most Important Subjects (Grant No. 2014YXQN01), 521 Talent Cultivation Program of Zhejiang Sci-Tech University (Grant No. 11110132521310) and Open Foundation of the Key Lab of Pulp and Paper Science & Technology of Ministry of Education, Qilu University of Technology (Grant No. KF201403).

References

- [1] C.H. Luo, J.Q. Qu, H.Q. Chen, *Acta Materiae Compositae Sinica*. **29** (2010).
- [2] Y. J. Tang, D. D. Zhou, J. H. Zhang, *Dig. J. Nanomater. Biostruct.* **8**, 1699 (2013).
- [3] Q. Q. Pei, Y. J. Tang, J. H. Zhang, X. M. Zhu, D. D. Zhou, *Dig. J. Nanomater. Biostruct.* **9**, 1407 (2014).
- [4] H.M. Etmimi, R.D. Sanderson, *Macromolecules*. **44**, 8504 (2011).
- [5] X.L. Tong, R.D. Wu, R.L. Wang, *Silicone Material*. **16**, 1 (2002).
- [6] D.M. Qi, Y.Z. Bao, Z.M. Huang, Z.Y. Wen, *Acta Polymerica Sinica*. **774** (2006).
- [7] Y.Y. Li, H.Q. Chen, X.J. Yang, L.D. Lu, X. Wang, *China Plastics Industry*. **31**, 37 (2003).
- [8] C.H. Duan, J.F. Zhou, Z.S. Wu, H.X. Dang, *Acta Physico-chimica Sinica*. **19**, 1049 (2003).
- [9] Y. Zhang, G.E. Zhou, L. Li, Y.H. Zhang, *Chinese Journal of Materials Research*. **12**, 291 (1998).
- [10] Z. Jia, G.S. Tian, Y.G. Yang, *Bulletin of the Chinese Society*. **28**, 940 (2009).
- [11] M.S. Huang, Y. Luo, X.M. Dong, G.Z. Deng, *Guangdong Chemical Engineering*. **4** (2009).
- [12] W.J. Wu, J.Y. Gu, H.Y. Liu, *Chemistry and Adhesion*. **345** (2006).
- [13] H.B. Liu, S.G. Wen, J.H. Wang, Z.X. Xu, W.Z. Chen, Y. Chen, P.P. Zheng, *Acta Chimica*

Sinica. 1930 (2010).

- [14] J. Zhang, X.R. Zhen, H.Q. Li, F.C. Zhao, Chemistry and adhesion. **34**, 9 (2012).
- [15] Z.Y. Yang, Y.J. Tang, J.H. Zhang, Chalcogenide Letters. **10**, 131 (2013).
- [16] Z.H. Fu, X.Y. Zhang, H. Huang, H.Q. Chen, Modern Chemical Industry. **24**, 62 (2004).
- [17] C.J. Wu, Q. Pang, A.M. Qin, C.J. Liang, Function Material. **44**, 3174 (2013).
- [18] L.H. Huang, K.F. Chen, C.X. Lin, R.D. Yang, R.A. Gerhardt, Journal of Materials Science. **46**, 2600 (2011).